COMPARISON OF TEXTURE ANALYSIS TECHNIQUES IN BOTH FREQUENCY AND SPATIAL DOMAINS FOR CLOUD FEATURE EXTRACTION

Nahid Khazenie[1,2]

[1]University Corporation for Atmospheric Research, Boulder, CO 80301

Kim Richardson[2]

[2]Naval Research Laboratory, Monterey, CA 93943-5006

ABSTRACT

Identification of cloud types through cloud classification using satellite observations is yet to produce consistent and dependable results. Cloud types are too varied in their geophysical parameters, as measured by satellite remote sensing instruments, to provide for a direct accurate classification. To aid in classification, texture measures are additionally employed. These measures characterize local spectral variations in images. They are widely used for image segmentation, classification, and edge detection. Numerous methods have been developed to extract textural features from an image on the basis of spatial and spectral properties of the image. In our effort, several of these methods are studied for their applicability in cloud classification and cloud feature identification. The examined texture methods include a) spatial gray-level co-occurrence matrices, b) gray-level difference vector method, and c) a class of filters known as Gabor transforms. Methods a) and b) are spatial and statistical while method c) is in the frequency domain. A series of comparative tests have been performed applying these methods to NOAA-AVHRR satellite data. A discussion as to the suitability of these texture methods for cloud classification concludes this study.

Key Words: texture analysis, cloud classification, Gabor transforms, spatial gray-level co-occurrence matrices, gray-level difference vector (GLDV), NOAA-AVHRR.

INTRODUCTION

Identification of cloud types by automated cloud classifiers, which operate on a pixel by pixel basis, has yet to show dependable and accurate results. Clouds have geophysical parameters which are too inconsistent, as measured by satellite remote sensing instruments, to provide for a direct accurate classification. No method developed to date provides a reliable spectral signature which would uniquely identify a specific cloud type anywhere on the Earth globe during any season. Cloud types vary in their spectral response at different latitudinal locations and at different times of the year. These variations complicate methods required for cloud type identification using remote sensing techniques.

Surveying the various available statistical, structural, and frequency domain techniques applied to cloud classification, it appears that there are not enough parametrization vectors to uniquely separate any one cloud type. For this reason, texture analysis methods are drawn upon in addition to aid in this problem. The use of texture parameters has been reported on extensively in recent literature (Wechsler, 1980). Texture techniques used in our study include a) spatial gray-level co-occurrence matrices, b) gray-level difference vector (GLDV) method, and c) a class of filters known as Gabor transforms. Each of these approaches has unique merit for providing additional information about cloud masses within a scene. These unique differences are the focus in this study.

Images in this case study are composites of Advanced Very High Resolution Radiometer (AVHRR) channel one and channel four. Pixel by pixel classifications of cloud types, based on the spectral and spatial responses from these channels, are enhanced with results from the various texture analysis algorithms. Results of the classifications from the combined techniques are compared and discussed.

DATA

An image from the Gulf of Alaska was chosen for this work. This region was selected due to its high latitude which presents challenging solar zenith angles. It also provides snow within the scene which tests snow and cloud separation capabilities of the candidate methods. Furthermore, the general meteorological activity within this region is high thereby presenting a continuous varying source of frontal cloud masses.

The scene selected for presentation is one of eight images used in this study. It is an AVHRR image from 15 October 1988, 19Z. A full resolution (**1.1** km per pixel) sector of **1024** by **1024** ten-bit pixels was extracted from the original **2048** by **2048** data set.

The channel one and channel four radiance images are shown in Figures 1 and 2. The channel one image is histogram-equalized for purposes of display. The channel four image is inverted so as to represent clouds in lighter gray shades.

The large band of clouds in the extreme right of the image is a frontal cloud mass that has previously moved through the area. This cloud mass is characterized by high thick cirrus over cumulus. These clouds are brightened by their height as well as by the low sun angle which is characteristic for this northern latitude.

In the lower central portion of the image are well defined cloud streets. They are trailed by open cell stratocumulus and altostratus that extend to the left center of the image. The mixed layered cloud mass in the lower left portion of the image represents stratus and altostratus with a cover of thick cirrus. Some closed cell stratocumulus are at the bottom of the image between the stratus and frontal clouds.

Snow can be seen in the upper central portion of the image. Typically, snow will be observed to have a dendritic-like structure which distinguishes it from cloud masses.

TEXTURAL METHODS

Texture is a term used to characterize the surface of a given object. It can also be applied to an image of a phenomenon. It is undoubtedly one of the main features drawn upon in image processing and pattern recognition. Texture analysis plays a fundamental role in classifying objects and outlining significant regions of a given gray level image (Wechsler, 1980). Despite its ubiquity in image data, though, texture lacks a precise definition. Some definitions characterize texture as visual images which possess some stochastic structure. Other definitions describe texture as an attribute generated by a local periodic pattern. Whatever the definition, most algorithms which derive texture from an image fall into the categories of either statistical or frequency domain. A brief description of the three texture methods of interest follows.

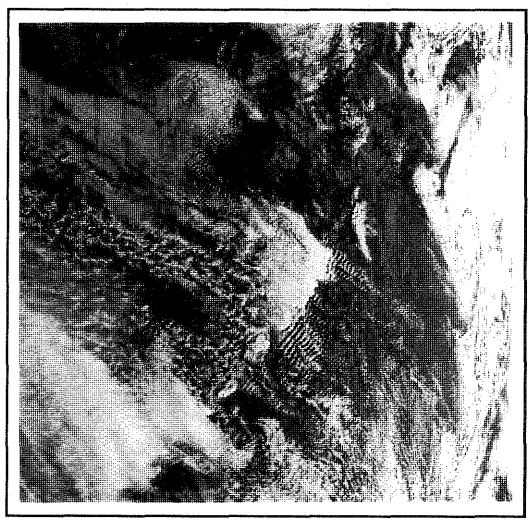

Figure 1. AVHRR channel 1 ten-bit radiance values, histogram equalized for display.

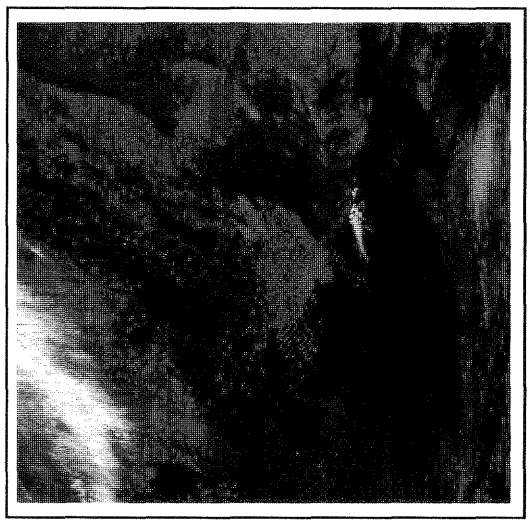

Figure 2. AVHRR channel 4 ten-bit radiance values, inverted for display.

Statistical Methods

The two most commonly used statistical texture methods are the a) gray-level difference vector (GLDV) method (Welch et al., 1990, Khazenie and Richardson, 1991), and the b) co-occurrence matrix method (Haralick, 1973). Our current study draws upon both of these methods. Both methods extract a set of statistical parameters from a given image. Some of the commonly extracted texture parameters are inertia, correlation, homogeneity, entropy, energy, variance, skewness, and kurtosis. These parameters are then used as the input features to a classifier.

Texture measures are derived commonly from statistical parameters of first or second order. The GLDV method estimates the probability density function for differences taken between image function values at locations spaced **d** pixels apart and at an angle θ. The resulting texture measures are based on this first order statistic. The spatial co-occurrence matrix method, on the other hand, estimates the joint gray level distribution for two gray levels located at a distance **d** and at an angle θ. The texture measures derived by the co-occurrence matrix method are based on this second order statistic.

The co-occurrence matrix method is used in this study to derive texture values of entropy, homogeneity, energy (similar to the GLDV angular second moment), and correlation. These four parameters were calculated for the radiances of each of the two channels, AVHRR channel one and channel four, for a total of eight texture values. Each texture value was processed using three different convolution sizes. The **n** by **n** convolution sizes are **n = 3**, **9**, and **16**. In addition, the search angle for each of the convolutions was varied to determine whether or not the derived textures possess any angular dependence. The angle was set to $\theta = \mathbf{0},^{o}\ \mathbf{45},^{o}\ \mathbf{90},^{o}$ and $\mathbf{135}.^{o}$ Search angle dependence is expected only when the surface resolution is much smaller than the **1.1** km surface resolution of the AVHRR instrument and indeed, as discussed later, no angular dependence was identified using the co-occurrence matrix method and the given image data.

The GLDV technique was similarly applied. The same texture values as for the co-occurrence matrix method were calculated. The calculations were performed on the same channel one and channel four radiance values, but only for a single search angle, $\theta = 0$. The search angle non-dependence had already been established from working with the co-occurrence matrix method. Seven convolution sizes were chosen to derive the texture values of entropy, local homogeneity, and angular second moment. The convolution sizes were **n = 3**, **5**, **9**, **11**, **16**, **32**, and **64**. From a previous study (Khazenie and Richardson, 1991) the three sizes of **n = 3**, **16**, and **64** provided the best statistical representation of the data for use in cloud classification. This finding was re-established in the current work.

Frequency Domain Methods

Spatial granularity and repetitiveness is one of the characteristic aspects of texture. Both can be quantified by looking at the frequency content of an image. It is therefore reasonable to expect that transform techniques are suitable for extracting texture information from images.

The Fourier transform analysis method (Lendaris et al., 1970) is a procedure which works in the frequency domain. It is, by far, the most used transform method. Image features, such as spectral rings or edges, are derived from the image power spectrum by this technique.

Related to the Fourier transform are functions first introduced by Gabor (Gabor, 1946). These functions have been extended

to two dimensions (Daugman, 1980) resulting in what is known as the two-dimensional (2-D) Gabor filters.

One of the unique properties of Gabor filters is their ability to discriminate textural features in a way similar to that of human vision (Fogel et al., 1989). Another important property is their achievement of the theoretical lower bound of joint uncertainty in the two dimensions of visual space and spatial frequency variables (Bovik et al., 1990). Additional advantages of Gabor transforms include their tunable spatial orientation, radial frequency bandwidths, and tunable center frequencies.

The 2-D Gabor filter is a harmonic oscillator, a sinusoidal plane wave within a Gaussian envelope. The convolution version of the complex 2-D Gabor function has the following general form.

$$G(x, y \mid W, \theta, \varphi, X, Y) = \left(\frac{1}{2\pi\sigma^2}\right) \cdot exp\left[\frac{-[(x-X)^2 + (y-Y)^2]}{2\sigma^2}\right] \cdot sin(W(x\cos\theta - y\sin\theta) + \varphi) \quad (1)$$

In equation (1), the Gaussian width is σ, the filter orientation is θ, the frequency is **W**, and the phase shift is φ. Variables **X** and **Y** define the center of the filter.

The Gabor function, equation (1), can be represented as a complex function having a real and an imaginary component, $\mathbf{G_1}$ and $\mathbf{G_2}$, respectively.

$$G_1(x, y \mid W, \theta, \varphi = 0, X, Y)$$

$$G_2(x, y \mid W, \theta, \varphi = \frac{\pi}{2}, X, Y)$$

Functions $\mathbf{G_1}$ and $\mathbf{G_2}$ are, respectively, even and odd symmetric along the preferred orientation direction θ. The results of convoluting $\mathbf{G_1}$ and $\mathbf{G_2}$ with any two-dimensional function are identical except for a spectral shift of $\pi/2$ along the direction θ.

Given an image **I(x, y)**, its Gabor transformation for a given filter size **n** with orientation angle θ and frequency **W** is given by the following equation.

$$S^2(X,Y \mid W,\theta) = [G_1 * I(x,y)]^2 + [G_2 * I(x,y)]^2$$

The Gabor filter described by equation (1) was applied to the AVHRR test images' channel one and channel four radiances. The response was evaluated for filters with θ = **0,° 45,° 90,°** and **135.°** The frequency **W** was set to $2\pi f/(n/2)$ where **f = 0.5, 0.6, 0.7, 0.8, 0.9,** and **1.0**. The tested filter sizes **n** were **9, 17, 33,** and **65**. The best results for cloud typing from the four convolutions was for **n = 17**.

RESULTS

The **1024** by **1024** ten-bit radiance data from channels one and four was used as input to the various texture algorithms. The texture output was then resized back to the full **1024** by **1024** resolution and added, as supplementary channels, to the radiance data. The resulting N channel data set was classified using a standard statistical unsupervised classifier.

Co-occurrence Matrix

The texture results from the co-occurrence matrix algorithm were first classified alone for each of the convolution sizes and search angles. Figure 3 is the result of this classification for an **n** by **n** convolution size where **n = 3** and for a search angle θ = **45.°** This represents the best result for all of the classifications from the co-occurrence matrix algorithm.

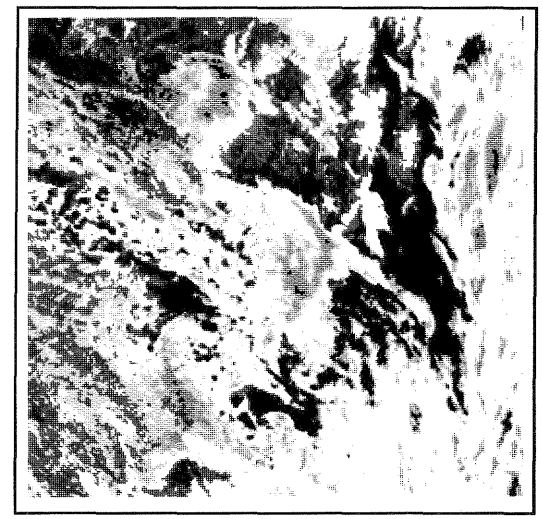

Figure 3. Texture values from the co-occurrence matrix algorithm, classified and scaled up for display.

It is clear from Figure 3 that the texture values alone do not represent cloud types with any accuracy. Figure 3 shows nine classes, but none identify any of the cloud types uniquely. The classified images are extremely noisy and at best represent features within the cloud masses rather than the cloud types themselves. There is, however, one reasonably accurate feature which resulted from this classification. For the lowest convolution size, at all search angles, the clear vs. cloudy areas are quite distinct.

For convolution sizes of **n = 9** and **16**, for all search angles, the classification separates the clear areas from the cloudy ones with success as well. It also produces a smoother classification. The cloud types, though, are still difficult to identify.

The classifications were performed twice on the texture results where **n = 9** and **16**. The first classification was performed on all of the texture values derived. The second classification was performed on the same values except for the correlation parameter. The results of the cloud type classification neither improved nor degraded. Therefore it seems that the correlation parameter does not contribute to the information needed for cloud typing.

In all cases of classifying only the co-occurrence matrix texture results, the thick cirrus was identifiable as a homogeneous feature, yet it was assigned the same class as portions of the open cell stratocumulus. Also in all cases, the snow was not separated from the clouds. The snow was assigned the same class as the stratus and altostratus clouds.

It was concluded at this point that classifying texture values alone does not provide sufficient results for identifying cloud types. The next step then was to provide more information to the classifier. The eight texture values were combined with the two AVHRR channel radiances (channel one and four) and classification was performed on the resulting ten channels of data.

The texture values for convolution size of **n = 9** were resized to the full **1024** by **1024** resolution, equal to that of the channel radiances, merged with the channel radiances, and the resulting data set was classified. The output is shown in Figure 4.

The search angle was varied as before, but the results from the classifier showed virtually no differences for unequal angles. The results for varied search angles were compared by calculating difference images. Only minor variations were noted in some of the mixed layer cloud types amounting for less than **1%** difference over the entire image. From this it was concluded that the process is not dependent on search angle and all further comparisons were made setting $\theta = \mathbf{0}.^{o}$

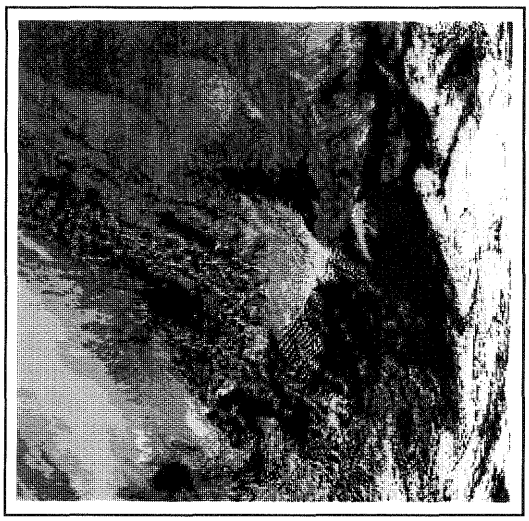

Figure 4. Combination of AVHRR channel 1, channel 4, and texture values from the co-occurrence matrix algorithm, classified.

The frontal cloud mass at the extreme right of the image in Figure 4 is represented by four distinct classes. The thick cirrus, the altocumulus, the cumulus, and the lower level stratocumulus each appear as distinct cloud types. They are affected by the sun angle thereby giving the cirrus over the frontal cloud mass a different class than the cirrus over the stratus in the lower left portion of the image.

The classes representing the stratus clouds provide more separation of cloud types than a human photointerperter would give. Should the goal be to duplicate human performance, one can easily combine some of the statistical classes. However, our goal was to obtain parameter vectors for performing unsupervised cloud classifications, no matter how many vectors there may be, as long as the distinct cloud types can be separated from each another. That goal was achieved.

Gray Level Difference Vector

The texture results from the gray level difference vector (GLDV) algorithm were first classified alone, identically as for the co-occurrence matrix. Similarly, the classification results from these texture values alone do not provide cloud type information directly. The results are essentially identical to those shown in Figure 3 for the co-occurrence matrix. The textures values, when classified, identify edges between features within the image well, but the features are various areas within the cloud type rather than the cloud type itself.

As with the co-occurrence matrix method, the GLDV performs very well at identifying cloud versus no cloud areas within the scene. It is not know at this time, however, if this capability can be extended easily to all AVHRR images. With more study this may indeed prove to be the case. Simple thresholding of the texture values may be all that is required. Results from a previous study (Khazenie and Richardson, 1991) support this conjecture.

As with the co-occurrence matrix output, the textures derived by the GLDV were then combined with the channel one and channel four radiances. The resulting eight channels were classified and the outcome is shown in Figure 5. Again, the results are essentially identical to those from the co-occurrence matrix method (Figure 4) in their ability to type clouds. Sun angle remains a problem within the frontal cloud region at the extreme right of the image. However, the mixed layer clouds in the lower left show the same successful level of cloud type separation as with the co-occurrence matrix method.

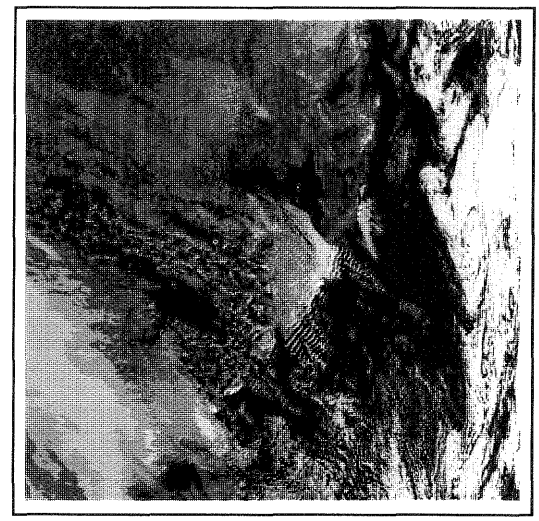

Figure 5. Combination of AVHRR channel 1, channel 4, and texture values from the GLDV algorithm, classified.

Convolution size plays a role in the ability to type clouds. For **n > 16** the algorithm is able to identify the presence of clouds. It is also able to determine that the texture in the region is unique. However, it does not provide enough information to the classifier to separate cloud types. Although the statistical significance is in favor of the higher convolution sizes, it is the lower convolution sizes that provide the textural significance to the classifier for cloud type identification.

Gabor Filters

Figure 6 presents the result of classifying the test image channel one and channel four radiances combined with the Gabor filter output where **n = 17** and phase angle $\varphi = \mathbf{0}$. Of the available **2048** by **2048** data, the same **1024** by **1024** scene was originally acquired as for the statistical methods. However, computer resources available for the study of Gabor filters could digest no more than **512** by **512** images. Therefore, only the lower left quarter of each **1024** by **1024** scene was analyzed. One such quarter is shown in Figure 6.

The thick cirrus over the stratus is well separated. This is a great improvement over the classification of texture values from the Gabor filter alone. Indeed the classifications of the combined image, radiances and textures shown in Figure 6, are much easier to label than are either of the classifications based on texture only.

Convolution sizes **n > 17** do not perform well for a wide variety of cloud types within a scene. This follows along with the same findings as for the statistical textural methods. Important textural attributes in the cloud mass are lost when

higher convolution sizes are used. With such convolution sizes, the textural analysis shows the dominant texture over each cloud mass, but does not sufficiently indicate characteristic features of that cloud mass thereby missing the classification of the cloud type. In particular, the open cell stratocumulus and altostratus within the image did not separate out at the higher convolution sizes.

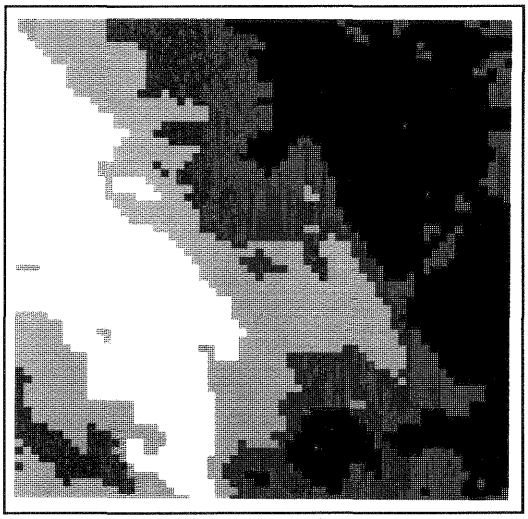

Figure 6. Combination of AVHRR channel 1, channel 4, and texture values from the Gabor filter, classified. The results shown cover only the lower left quarter of the test image.

While it has not been tested in this study directly, it is conjectured that the approach using the Gabor filter will be less sensitive to latitude variances and seasonal changes compared to the two statistical techniques. The Gabor filter is a tunable algorithm. With proper adjustment of control parameters it should be possible to desensitize the filter to local effects, such as latitude changes and seasonal effects, while retaining the ability to extract the required physical response which uniquely represents each cloud type.

Inter-comparisons

The results from classifying only the output of the two statistical textural methods, the co-occurrence matrix and the GLDV, are almost exactly alike. This is reasonable since the texture measures calculated by both of these algorithms were the same. One should expect the same results even though they were arrived at by different means. The GLDV is based on first order statistics while the co-occurrence matrix method is based on second order statistics. It can therefore be concluded that, given our test images, the extra complexity of the second order statistics is not necessary for arriving at satisfactory results.

It is also noteworthy that the results from the two statistical methods are virtually identical even though different convolution sizes were used. This suggests that the features, which distinguish cloud types, are fairly coarse. It also suggests a lack of fine features which would distract a method that uses a small convolution size.

The output of the Gabor filter has different characteristics compared to the output of the co-occurrence matrix and GLDV, yet the ability to separate cloud types is very similar for all three methods. The resolution of the Gabor filter output is lower, seventeen pixels versus nine for the co-occurrence matrix and three for the GLDV. The classification results are greatly influenced by this resolution difference. This is obvious by comparing the pixel size in Figure 6 with Figure 4.

In Figure 6 the boundary of the thick cirrus over the stratus has been smoothed. This is also true for the stratus cloud types. The separation of multilayered clouds is similar for all three methods.

The computer processing time required for the Gabor filter method proved much less than either of the two statistical methods (co-occurrence matrix or GLDV). Processing a full **1024** by **1024** scene using the Gabor filter took approximately one minute on a SUN SparcStation II. The statistical methods required approximately ten minutes each for the same image.

CONCLUSION

Classification of cloud types using spectral and derived textural parameter vectors alone has not been completely successful. Additional information about texture in the image provides more input to a cloud classifier. Such an addition shows considerable improvement over cloud classification based only on spectral information. Despite the marked improvement, however, it does not yet appear that the addition of texture information provides all of the necessary parameters required to successfully classify and completely label cloud types. Nevertheless, results from this study indicate that Gabor filters applied to the spectral data set, and used in conjunction with the spectral data for classification, extract cloud types better and faster than the other techniques explored.

Acknowledgements

The authors extend their extreme appreciation to Mr. Mike Linda for his invaluable help and fortitude.

The NRL Contribution number is 92:087:431. The authors gratefully acknowledge the support of the sponsor, the Office of Naval Technology, Code 22, Mr. James Cauffman, Program Element 62435N. This paper is approved for public release; distribution is unlimited.

REFERENCES

Bovik, A. C., M. Clark, and W. S. Geisler, 1990. Multichannel Texture Analysis Using Localized Spatial Filters. *IEEE Trans. on Pattern Anal. Machine Intell.*, 12(1):55-73.

Daugman, J. D., 1980. Two Dimensional Spectral Analysis of Cortical Receptive Field Profiles. *Vision Res.*, 20:847-856.

Fogel, I., and D. Sagi, 1989. Gabor Filters as Texture Discriminators. *Biological Cybernetics*, 61(2):79-162.

Gabor, D., 1946. Theory of Communication. *J IEE*, 93:429-457.

Haralick, R. M., K. Shanmugam, and I. Dinstein, 1973. Textural Features for Image Classification. *IEEE Trans. Systems, Man and Cybernetics*, SMC-3(6):610-621.

Lamei, N., N. Khazenie, and M. M. Crawford, 1992. Multi-Spectral Texture Analysis for Cloud Feature Discrimination. *Proc. IGARSS'92 Symp.*, May 1992, Clear Lake, Texas.

Lendaris, G. O., and C. L. Stanley, 1970. Diffraction Pattern Sampling for Automatic Pattern Recognition. *Proc. IEEE*, 58(2):198-216.

Khazenie, N., and K. Richardson, 1991. Classification of Cloud Types Based on Spatial Textural Measures Using

NOAA-AVHRR Data. *Proc. IGARSS'91 Symp.*, 3:1701-1705.

Wechsler, H., 1980. Texture Analysis -- A Survey. *Signal Processing*, 2:271-282.

Welch, R. M., K. Kuo, and S. K. Sengupta, 1990. Cloud and Surface Textural Features in Polar Regions. *IEEE Trans. on Geoscience and Remote Sensing*, 28(4):520-528.